Experimental Physics 3: Experiment II
X-ray spectroscopy, attenuation and diffraction

Group B
Andreas V. Flarup 202006446
Andreas S. Niebuhr 202005667
Rasmus L. Mikkelsen 202005762
Kristoffer I. R. Pedersen 202009792
IFA Aarhus University

Abstract

This report covers three experiments with X-rays interacting with matter using an Amptek silicon drift X-ray detector. The X-ray is first used to determine the type and thickness of three absorbers. It is shown that the absorbers are Mo, Ag, and Au. The thickness of them were measured to be $x_{\text{Mo}} = 23.5 \pm 3.8\mu m$, $x_{\text{Ag}} = 21.3 \pm 4.0\mu m$ and $x_{\text{Au}} = 30.0 \pm 4.0\mu m$. Then the X-ray fluorescence of meteorites were measured to determine the iron/nickel ratio in them. Three different meteorites were looked at named 'Shining Meteorite', 'Spotted Meteorite', and 'Diablo Canyon Meteorite'. It is concluded that the iron/nickel ratios are $\left(\frac{N_{\text{Fe}}}{N_{\text{Ni}}}\right)_{\text{Shining}} = 11.10 \pm 0.01$, $\left(\frac{N_{\text{Fe}}}{N_{\text{Ni}}}\right)_{\text{Spotted}} = 22.5 \pm 0.1$ and $\left(\frac{N_{\text{Fe}}}{N_{\text{Ni}}}\right)_{\text{Diablo Canyon}} = 15.26 \pm 0.08$. Lastly peaks from a crystal coming from Laue diffraction were observed and it was concluded that the peaks clearly follow a linear function. It was possible to measure the distance between the planes which was measured to be $d = 1.04\text{nm} \pm 0.05\text{nm}$.

1 Introduction

In this exercise some properties of X-rays are investigated. X-rays can be made in a couple of different ways however the most common is by accelerating electrons which then collide with a target making the electrons release X-rays. X-rays were first discovered by Röntgen in 1895 and they have a wavelength of 10^{-8} to 10^{-11} m. X-rays are useful for a number of different things. For instance they can be used in radiography where it is possible to make an image of the human body to look for fractures in the bones or to look at your teeth. They can also be used in radiotherapy to cure some forms of cancer. By shooting x-ray at different absorbers one may identify them by looking at their absorption edges and deduce their thickness. The iron to nickel ratio in metallic meteorites will also be determined by using X-ray fluorescence. The Laue diffraction will also be investigated to deduce the spacing between diffraction planes in a crystal.

2 Theory

2.1 X-ray production

In practise the X-rays are made from an X-ray generator with a copper cathode. A strong elec-

tric field up to 36 kV in our experiment accelerates the electrons inside the generator. When they finally hit the target and is slowed down drastically, photons with high energies are emitted. As we shall later see the two characteristic lines K^{α} and K^{β} from Cu results in visible peaks, which is a consequence of the X-ray generators properties.

2.2 Silicon drift detector

The experiment uses a silicon drift detector to detect the X-rays. When a photon hits the silicon between the anode and cathode in the detector, it ionizes the silicon. The uniform electric field between the anode and cathode then exerts a force on the ion, moving it to the diode where it is collected. This creates a current pulse which is then amplified and eventually send to the computer. The detector used in this experiment is the SDD-amtek, which has a high energy resolution even at high count rates.

2.3 X-ray interaction in matter

When X-rays hit matter it can mainly interact with it in three different ways. The first is the photoelectric effect where an atom in the matter absorbs the incoming photon γ and emits an electron e^{-}. The probability P for the interaction to occur scales approximately as

$$P \propto \frac{1}{E_{\gamma}^{3}}$$

where E_{γ} is the energy of the incoming photon. One of the non negligible effects are the absorption edges which is a dramatic decrease in intensity at a specific energy level. They occur at energies matching a given shell energy in the atom. From energy conservation we get

$$T_{e^-} = E_{\gamma} - B_{e^-}$$

Where T_{e^-} is the kinetic energy of the electron and B_{e^-} is the binding energy of the electron in a given shell. So for photoelectric absorption to occur we must have

$$E_{\gamma} \geq B_{e^-}$$

It is seen that when E_{γ} just exceeds one of these energies it is also possible for the photon to kick out electrons from the new shell. Therefore P increases dramatically at the energies matching the binding energy from a new inner shell. Since the energy levels in an atom is typically characteristic, one can, by finding the absorption edges in a spectrum, identify the atom.

The second effect of interest for the experiment is Compton scattering, where a photon scatters on a weakly bound electron so the electron escapes the atom while the now outgoing photon has less energy and changes direction. A Compton scattering has occurred when the scattered angle for the photon differs from 0 meaning the photon has interacted with the electron. The Compton scattered photon will not hit the detector together with the beam since the photon has changed direction. So Compton scattering will also have an effect on the experiment, however it is more dominant at higher energies. In fact the relative domination of the three effects depends both on energy and the proton number Z. For instance at $Z = 20$ Compton effect is dominant for energies between 100keV and 10MeV [1].

The third interaction is pair-production. Here a photon produces a electron-positron pair and disappears. Neglecting the kinetic energy of the

atom present to ensure conservation of momentum we get

$$E_\gamma = T_{e^-} + T_{e^+} + 2m_e c^2$$

where T_{e^+} is the energy of the positron, m_e is the mass of the electron, and c is the speed of light. This gives the condition $E_\gamma \geq 1\text{MeV}$. Therefore the effect is irrelevant for this experiment.
The total probability for the one of the interactions to occur is just the sum of the contributions for each effect. And since they all scale with the thickness of the material one can define μ as the total probability for an interaction to happen per unit length. The number of photons hitting the detector is the incoming number minus the number of photons which interacted. Therefore we get the exponential decrease in I, the intensity,

$$I(x) = I_0 e^{-\mu x} \tag{1}$$

Where x is the thickness of the material and I_0 is the intensity at $x = 0$. And μ is of course greatly depended on E_γ due to the individual effects' complicated dependence on E_γ see [1]. μ is called the linear attenuation coefficient and is unique for each material.

2.4 X-ray fluorescence

The photons in X-ray light have high enough energy to excite electrons in the inner orbitals. When it happens the electron structure becomes unstable, since one of the strongly bound electron orbitals is now available. An electron from an outer orbital can now jump spontaneously to the available inner orbital. Since the energy difference is so large, the emitted photon will be in the X-ray range. The precise energies of photons emitted in this way is characteristic for the atom, given that the incoming photon has high enough energy to excite the most tightly bound electron. Otherwise some of the peaks will be missing, but they will never change energy.

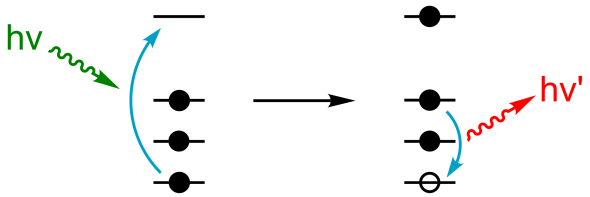

Figure 1: The excited atom can spontaneously decay to ground the ground state while emitting a photon with high energy see [2].

2.5 X-ray diffraction

We will also be looking at a special case of Laue diffraction called Bragg-Laue interference. When the light hits a crystal the reflected light emitted from different crystal planes can interfere. As can be seen on figure 2 the light reflected from the lower plane travels a distance of $2d\sin\theta$ longer than the other, where d is the distance between the two neighbouring planes. For constructive interference to occur we must have

$$2d\sin\theta = \lambda n$$

Where λ is the wavelength and the integer n is introduced to make sure the two beams are in phase at the detector. This condition also applies when the two planes are not neighbours since the distance always will be an integer multiple of d, which then goes into the n in Bragg's law.
From $E_\gamma = hc/\lambda$ we get the expected places of peaks in the energy spectrum as

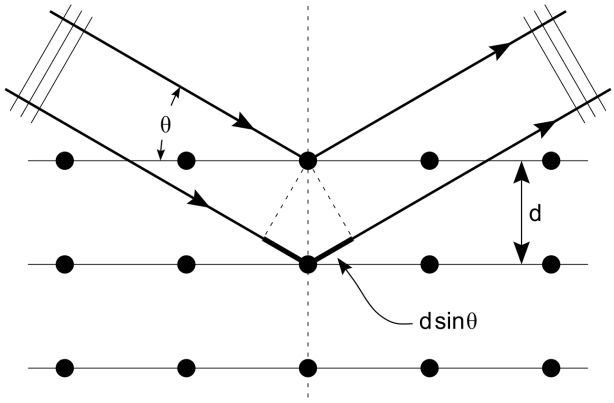

Figure 2: The light beam reflected from the lower plane lags behind with $2d\sin\theta$ [3]

$$E = \frac{hc}{2d\sin(\theta)}n \tag{2}$$

And it is seen that we expect an even spacing between the peaks due to Laue diffraction, and the spacing d between the planes can be found in this way [3]. In practise we will in this experiment place the detector at an angle of 90° to the beam, and therefore we will only see the effect, when the angle between the normal of the crystal and the beam is $\theta = 45°$, assuming the incoming and outgoing angle is the same. The effect is still present at $\theta \neq 45°$, but the detector should be placed in another angle to observe it. By taking advantages of this restriction we can then measure only the fluorescence peaks characteristic for the crystal at $\theta \neq 45°$ and both kinds of peaks at $\theta = 45°$. And one can then identify the peaks from the Laue diffraction and analyze them separately.

3 Experimental setup

The experiment was conducted using the X-ray generator with an Amptek Silicon drift x-ray detector at the end, which can be seen on figure 3.

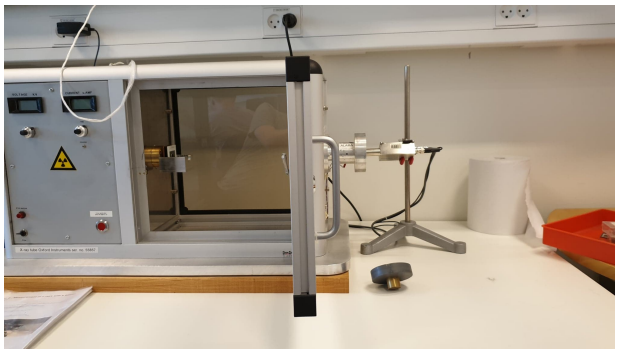

Figure 3: The x-ray generator and the detector. In the setup for the experiment the detector was pointed as seen on the picture or at a 90° angle with respect to the generator.

The detector was connected to a computer where by using the software dppMCA (see [4]) it was possible to see the number of counts that were detected as a function of the channel number of the detector. The detector was put in two different places depending on what part of the experiment was done: at a 0° angle with respect to the X-ray generator and at a 90° angle with respect to the X-ray generator.

3.1 Calibration

Since the detector is measuring as a function of channel number, a calibration is needed to convert the channel number to an energy.
For the energy calibration, the aforementioned setup was not used. Instead, the detector was

pointed at different sources, as seen in figure 4.

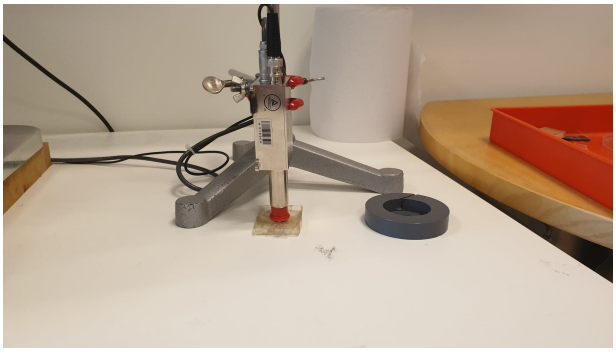

Figure 4: The detector is pointed at a source. From this data it is possible to calibrate the equipment.

From the sources it was possible to make a calibration from the channel number in the detector to energy. There was three different sources used: ^{55}Fe ^{137}Cs, and ^{241}Am each with several known peaks in the energy spectrum. The calibration was made from 5 min measurements.

3.2 Determination of thickness of absorbers

For this part of the experiment the absorbers were placed in the chamber of the X-ray generator (see figure 5).
In this part of the experiment a collimator should be in the chamber with the absorbers to make the X-rays travel parallel with respect to the detector. The X-rays therefore travel in the same direction directly towards the detector. The measurements were 10 min. in length with a voltage of 36kV and a current of 1 µA. A measurement was also made with no absorber first to get the spectrum of the X-ray beam alone. As seen from eq. 1 the

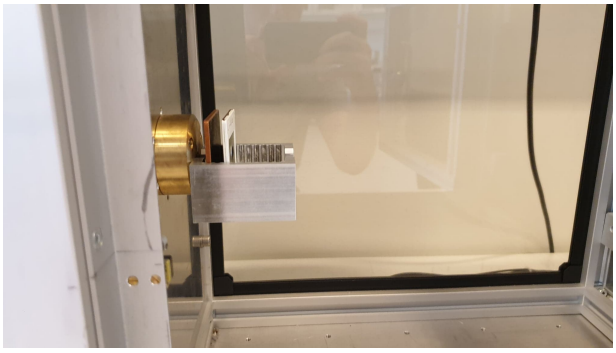

Figure 5: An absorber is placed inside the chamber of the X-ray generator. A collimator is also there.

initial intensity I_0 has to be known to estimate the thickness.

3.3 Determination of Fe/Ni ratios in meteorites

For this section, the detector should be put in a 90° angle with respect to the X-ray generator (Figure 6).
This is because the photons hit the front of the meteorites or calibration metals and therefore mainly excite electrons in the atoms at the incoming beam side of the material. Since the fluorescence effect is isotropic seen from the atom we can just put the detector such that the emitted photon does not have to travel through the rest of the object. Consequently we avoid loss of intensity due to this travel effect, and we obtain a lot more counts at the detector. Here a measurement of two different plates with a different ratio of iron to nickel is made as well as a measurement of the different meteorites. These measurements were 5 min. long with a voltage of 36kV and a current of 20µA. The collimator was

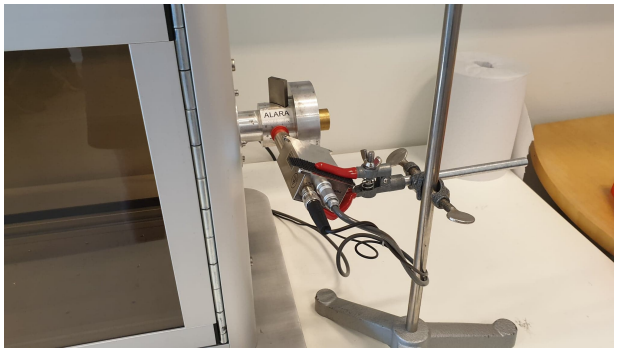

Figure 6: The meteorite is sitting at an angle making it so the detector also has to change place. The collimator is now removed to get more X-rays to hit the meteorite.

also removed as the X-rays no longer needed to travel in the same direction since we are looking at X-ray fluorescence.

3.4 Laue diffraction

This part of the experiment follows the same setup used for the meteorite, but instead of using a meteorite, the Muscovite glitter crystal was used. It was however put in the same place as the meteorite and measurements were made when the crystal was at 45° and when not at 45°. The measurement was 5 min long and a voltage of 36 kV and a current of 20 µA was used.

4 Data

4.1 Calibration

Calibration was done by looking at the peaks in the spectrum of the different known sources: ^{55}Fe,^{137} Cs and ^{241}Am. We found the channel number of the peaks since those energies have a table value. The peak was found by fitting a Gauss curve around it, thereby finding the channel number of the peak while also considering the points around. As can be seen on figure 7, there clearly is a linear relation between the energy and the channel number. This is described by the function $n(E) = (67.2 \pm 0.4)\text{keV}^{-1}E - 49 \pm 5\text{keV}$, where n is the channel number. An example of how a Gaussian function fitted to a peak is shown in figure 8.

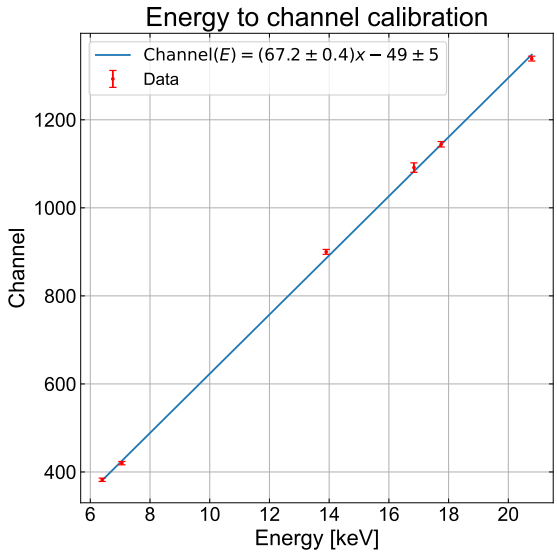

Figure 7: Calibration of energy in keV to the channel number. The uncertainties comes from the spread in the Gaussian fits.

4.2 Absorbers

The absorption edges can be seen in both figure 9 and table 1 with their respective energies. In table 1 the assumed metal each absorber is made

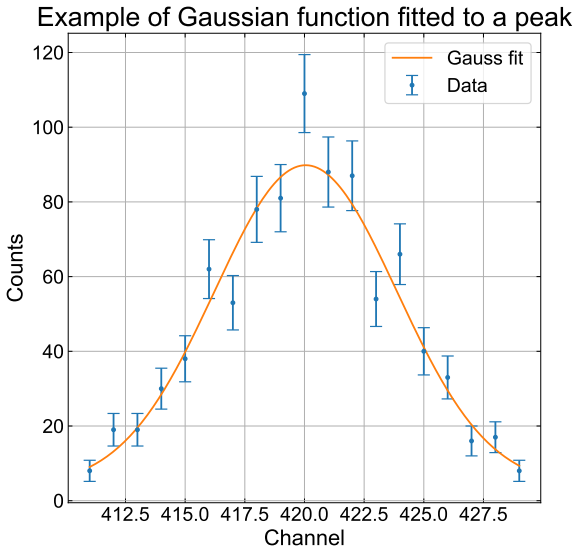

Figure 8: Example of how a Gaussian function is fitted to a peak.

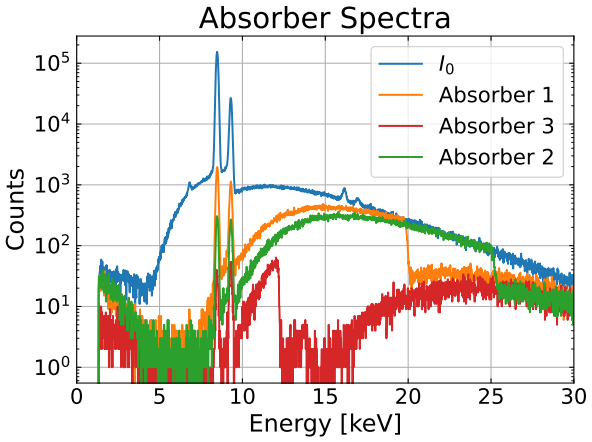

Figure 9: The measured intensities of the three absorbers and the reference intensity. The K^α and K^β lines are seen in all of the measurements including the one without absorber, since its origin is from the copper in the X-ray generator.

out of can also be seen, as well as the metals edge energies.

Abs	Edge[keV]	Metal	Edge[keV]
1	20.0 ± 0.1	Mo	20.0
2	25.3 ± 0.3	Ag	25.5
3	12.4 ± 0.1,	Au	12.0,
	13.8 ± 0.3,		13.7,
	& 14.5 ± 0.2		& 14.4

Table 1: The absorbers and the presumed metals with their respective edge energy. All the absorber energies lie close to the energies of their respective metal. The edge energies for the metals are from [5].

These metals are assumed because the K-edge energy for absorber 1 and Mo and absorber 2 and Ag lies pretty close. The L-edge energies for absorber 3 and Au also lies close. Furthermore absorber three is gold coloured which also confirms that absorber 3 is gold.
Since the absorbers could be identified, the μ coefficients can be taken from [6] by the use of the found energy - channel relation. From here, the thickness of the absorber at each energy can be extracted by

$$x = \frac{\ln\left(\frac{I_0}{I}\right)}{\mu(E_\gamma)}$$

at each energy value, where eq. 1 has been rewritten.
Results are seen in table 2.

4.3 Meteorites

When normalizing, as seen in figure 11, it is seen that the two fluorescence peaks to the left is at the same height while the right peak is lower for

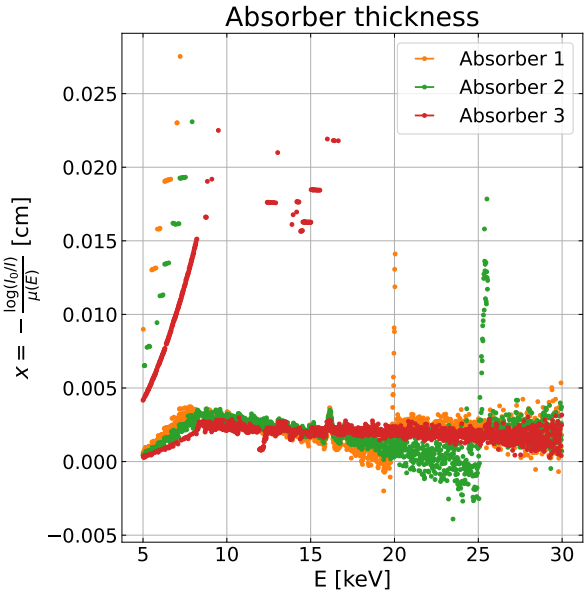

Figure 10: The corresponding thickness of the absorber at each energy point.

Absorber	Data [μm]	Tabel [μm]
1	23.5 ± 3.8	33
2	21.3 ± 4.0	30
3	30.0 ± 4.0	25

Table 2: The thicknesses is measured to be just within 3σ of the tablel value for arbsorber 1 and 2, while the accuracy is a little better for arbsorber 3.

Meteorite	Fe/Ni
Shining	11.10 ± 0.07
Spotted	22.5 ± 0.1
Diablo Canyon	15.26 ± 0.08

Table 3: The found values of iron to nickle ratios.

36% Ni. So we conclude that the two left peaks is from iron in the reference metal and the right is from Ni.

After the different peaks are identified we can distinguish the peaks in the meteorites and thereby find $I_{\text{Fe}}/I_{\text{Ni}}$ in them, which is the ratio of intensities.

Assuming a linear correlation between $I_{\text{Fe}}/I_{\text{Ni}}$ and $N_{\text{Fe}}/N_{\text{Ni}}$, which is the ratio of the amount of iron and nickel respectively, we can find the $N_{\text{Fe}}/N_{\text{Ni}}$ ratios in the meteorites. See figure 13 and table 3 for our findings. To account for extrapolation, uncertainties $\sigma_{N_{\text{Fe}}/N_{\text{Ni}}}$ were found by taking lower cone value at $I_{\text{Fe}}/I_{\text{Ni}} - \sigma_{I_{\text{Fe}}/I_{\text{Ni}}}$ and upper cone value at $I_{\text{Fe}}/I_{\text{Ni}} + \sigma_{I_{\text{Fe}}/I_{\text{Ni}}}$ and finally divide by 2.

4.4 Laue diffraction

By measuring both at $\theta = 45°$ and at $\theta \neq 45°$ we can compare the results and find the peaks due to Laue-diffraction since only the fluorescence peaks is present both times, as can be seen in figure 14. Finally the peaks only coming from diffraction can be plotted see figure 15.

It is seen that the data follows a straight line and is described by the function,

$$E = (0.84 \pm 0.04)\text{keV}\ n - 9.20 \pm 0.07\text{keV}$$

where n is the peak number. By using equation 2 we can find the spacing between the planes.

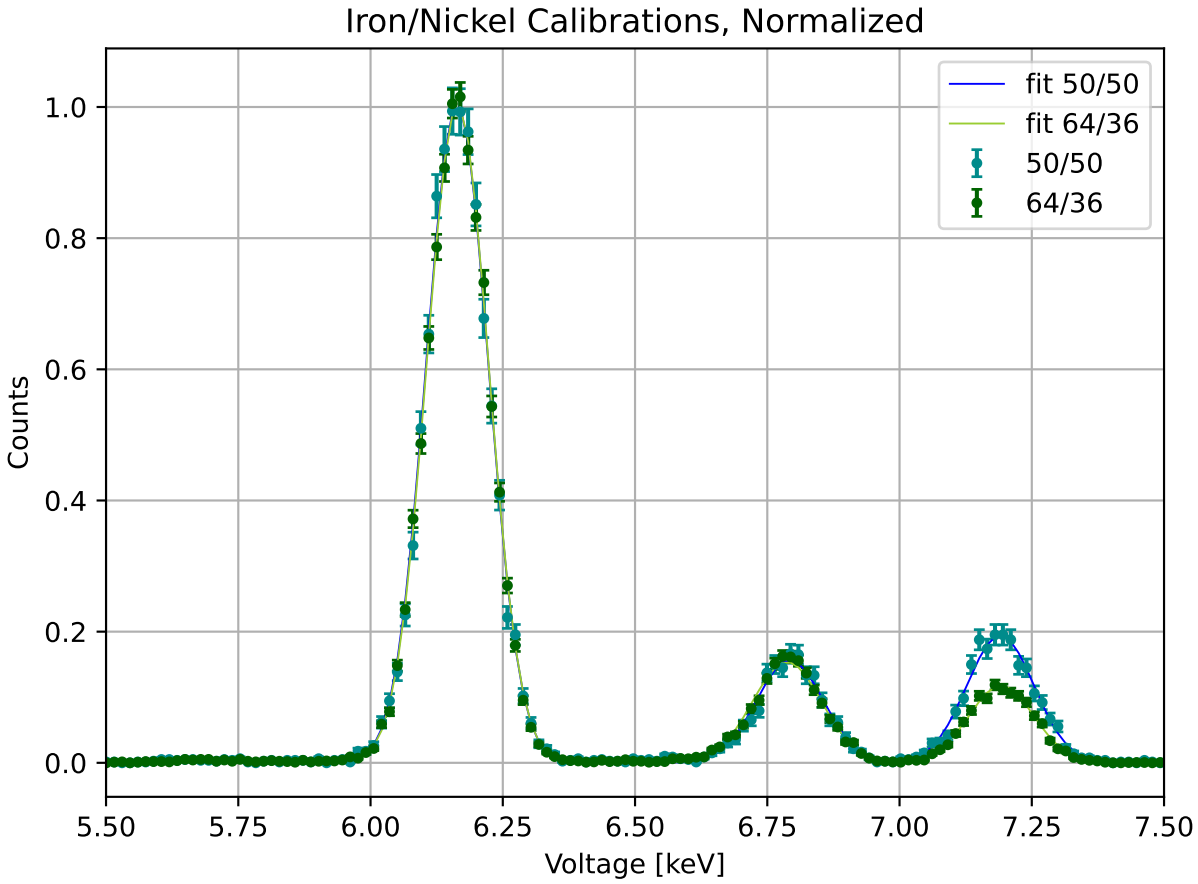

Figure 11: Part of the normalized spectrum of the two calibrations with 50/50 Fe/Ni (blue) and 64/36 Fe/Ni (green).

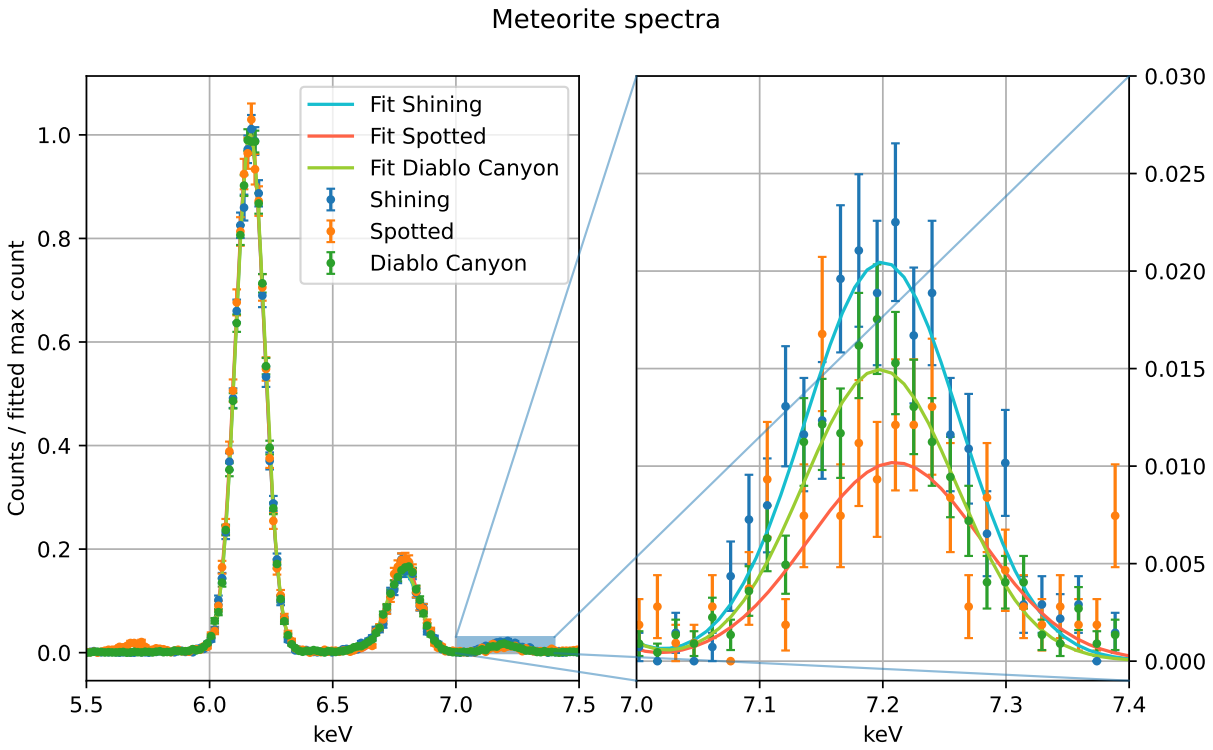

Figure 12: The spectrum from our three meteorites, focused around the three Fe and Ni lines. It should be clear, that the Ni peaks are very small and not far apart, revealing that there is a lot more iron than nickel in all of the meteorites, but the ratios still differs a lot.

The result is

$$d = 1.04\text{nm} \pm 0.05\text{nm}$$

The table value for the spacing is $d = 1.41$nm.

5 Discussion

5.1 Uncertainties

In general we had low uncertainties in our measurements. We used $\sigma_N = \sqrt{N}$ on the count number N in each channel since we can assume the count number is Poisson distributed. But the data points matched a Gaussian curve so well that we often lost a factor of 10^2 in the uncertainties in the height of a peak after the fit. So even after error propagation, the uncertainties were low. It also worked better when the energy position of the peak should be determined, since the Gaussian fits give very accurate σ values in the position of the peak.

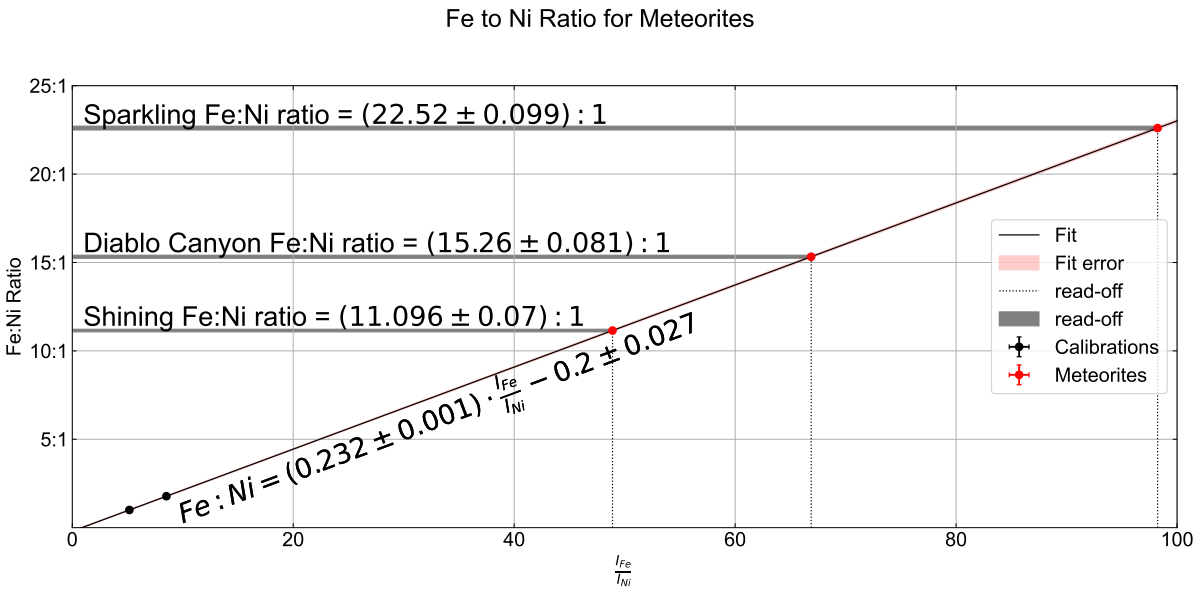

Figure 13: By extrapolating the linear model from the two known Fe-Ni metals we obtain N_{Fe}/N_{Ni} values for the meteorites. The error bars are too small to be seen.

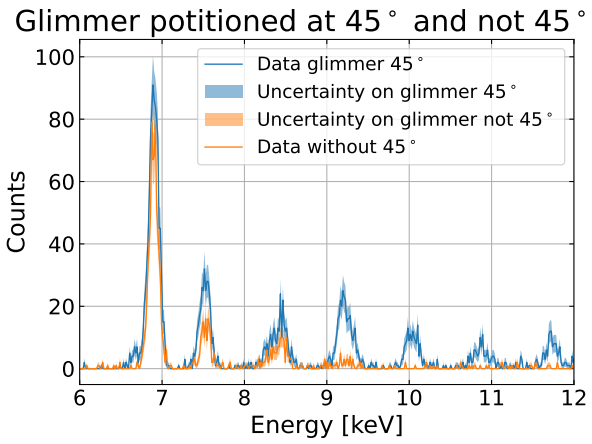

Figure 14: The raw data of the Muscovite crystal placed at 45° and not at 45°. The peaks due to Laue diffraction are only present at $\theta = 45°$.

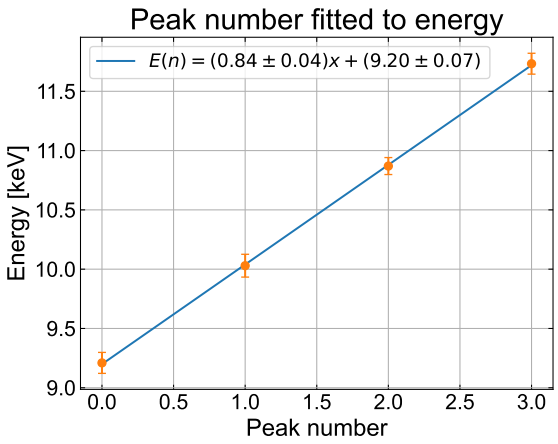

Figure 15: The acquired energy of the peaks found in the diffraction spectrum is fit to the corresponding peak numbers.

5.2 Absorbers

It was important to set the voltage to 36kV to get photons with energies in the entire range up to 36keV. We were not aware of that the first two times so we did not get the absorption edge for the silver absorber. And also the wider spectrum of E_γ simply gives more different measurements of the width. There are two problems with the results. As seen in 10 we get a big increase in x just before the edges. This indicates that there has been a systematic error in the channel to energy conversion so that the edges in our data lies at slightly lower energies. Therefore it does not fit with the table value of μ which we used in the calculation of x. This could be because we did not have time for calibration measurements at the third lab session where the data was taken and somehow a systematic offset was present that time. Also one could improve this problem by getting more and better calibration sources. Especially the ^{137}Cs had low activity so we could not use it in the channel to energy conversion. This is unfortunate since its lines are in the higher end of the energy and therefore of great importance for the slope in ch(E).

The other obvious problem is that we seem to get negative x values before the edges for Mo and Ag. This is due to the fact that we apparently measured larger values of I than I_0 as seen in figure 9. And accordingly $\ln(I_0/I) < 0$ in the calculation. Even though we were careful not to change the current during the experiment it still fluctuated a little. Therefore we might somehow have been unlucky with higher average current in the I measurement. We measured the absorbers in 10 min to try to let the current fluctuations average out. But since we only had the issues in the regions before an edge it hints that it is another systematic error maybe from the imprecise channel to energy conversion.

Analytically the experiment is very sensitive to small values in I, I_0 and μ. It is seen in figure 10 where we have some extremely large values of x when we have been dividing by a small number. Also in error propagation one can, by neglecting σ_μ, find

$$\sigma_x = \frac{1}{\mu}\sqrt{\frac{I_0 + I}{II_0}}$$

Which again is very sensitive to small values. So all in all the experiment is very sensitive to systematic errors e.g. in channel to energy conversion, and unfortunately we had some systematic errors in the experiment.

The known thicknesses of the absorbers are $x_{T_1} = 33\mu m$, $x_{T_2} = 30\mu m$ and $x_{T_3} = 25\mu m$ for absorber 1, 2, and 3 respectively. It is seen that we are within 3σ for Mo and Ag and just outside 1σ for Au for the thickness.

5.3 Meteorites

The uncertainties in the $N_{\text{Fe}}/N_{\text{Ni}}$ result are unreasonable low. The problem is, as discussed under the uncertainties section, that the Gaussian fit gives really low uncertainties on the height of the peaks and since we only have two calibration points the uncertainties in the linear fit are low. So even though we extrapolated really far away from the calibration metals, the uncertainties in $N_{\text{Fe}}/N_{\text{Ni}}$ still was low. If $N_{\text{Fe}}/N_{\text{Ni}}$ in the calibration was closer to the ones in the meteorites we could have measured it precisely however extrapolating always gives rise to uncertainties. Unfortunately we are not able to confirm our findings, as we have not found any published data on the Fe/Ni-ratios.

When looking closely at figure 12 it seems like the Ni peak for the Spotted meteorite is a little

randomized. This could lead to an error in our findings, and should we do the experiment again, we would definitely give that a longer exposure to get rid of the randomness and get a better Gaussian fit.

5.4 Laue diffraction

As seen in figure 14 we found 4 peaks due to Laue diffraction since they were not present at $\theta \neq 45°$. One could argue that there actually is a small peak for $\theta \neq 45°$ at the first of the Laue peaks at $E = 8.5$keV. But since this is very small compared to $\theta = 45°$ it should be a little Laue diffraction effect, since the fluorescence does not depend on the angle. It can be concluded that the data follows the linear relation very well. However it is clear that there must have been a systematic error in the experiment. This is because we are 8σ from the table value, but the fitted function goes through the error bars anyway, see figure 15. Should the experiment be performed again one should first of all see if the results still yields the result of $d = 1.04 \pm 0.05$nm. One could also try to measure some of the other crystals which would indicates whether the systematic error is special for the Muscovite crystal, or it is more likely to be in the setup.

6 Conclusion

Based on our work with the experiment we can conclude that the absorbers have thickness $x_1 = 23.5 \pm 3.8\mu$m, $x_2 = 21.3 \pm 4.0\mu$m and $x_3 = 30.0 \pm 4.0\mu$m. The uncertainties of these values do not encompass the table values, likely due to systematic error.
From the meteorites we can conclude that they each contain a very small amount of nickel compared to iron. For the shining, spotted, and Diablo Canyon meteorite the iron to nickle ratios was $\left(\frac{N_{\text{Fe}}}{N_{\text{Ni}}}\right)_{\text{Shining}} = 11.10 \pm 0.01$, $\left(\frac{N_{\text{Fe}}}{N_{\text{Ni}}}\right)_{\text{Spotted}} = 22.5 \pm 0.1$ and $\left(\frac{N_{\text{Fe}}}{N_{\text{Ni}}}\right)_{\text{Diablo Canyon}} = 15.26 \pm 0.08$ respectively.
We can conclude that Laue diffraction exists since we were able to measure several peaks not from fluorescence at $\theta = 45°$ but from Laue diffraction. We did also find the predicted linear dependence of energy as a function of peak number very clearly. We found the spacing between the planes in the Muscovite glitter crystal to be $d = 1.04\text{nm} \pm 0.05\text{nm}$, which seems to be in a reasonable size order.

References

[1] Kenneth S. Krane. *Introductory Nuclear Physics.*

[2] *Wikipedia X-ray flourescence.* URL: https://en.wikipedia.org/wiki/X-ray_fluorescence.

[3] *Wikipedia Bragg-Laue diffraction.* URL: https://en.wikipedia.org/wiki/Bragg%5C%27s_law.

[4] *Software guide (dppMCA).* URL: https://brightspace.au.dk/d2l/le/lessons/71471/topics/1015741.

[5] *Absorption edges.* URL: https://www.ruppweb.org/Xray/elements.html.

[6] *Linear attenuation coefficients.* URL: https://physics.nist.gov/PhysRefData/FFast/html/form.html.